Morphological and functional evaluation of angiogenesis of a xenografted human sarcoma in nude mice

Christoph Pöttgen[1], Gero Hilken[2], Udo Vanhoefer[3], Martin Stuschke[1] and Georg Stüben[1]

[1]Department of Radiotherapy; [2]Central Animal Laboratory; [3]Department of Internal Medicine/Cancer Research, University of Duisburg-Essen Medical School, Essen, Germany

Summary

The implantation of tumour cells in normal tissues and the subsequent induction of angiogenesis by the growing xenograft were studied by means of immunohistochemistry and digital image analysis. Tumour growth was induced by injection of a human spindle cell sarcoma (ES3) into the subcutis of HsdCpb:NMRI-*nu/nu* mice. *In vivo* injection of Hoechst 33342 was used as a marker of perfusion. The vasculature was stained with specific antibodies and subsequently analysed by digital image analysis. Starting at day 3 up to day 6, angiogenesis could be detected and the relative amount of perfusion within the investigated area reached a peak at day 6. This method, which allows investigation of both functional and morphometric characteristics of human xenograft vasculature, serves as an excellent assay for evaluation of antiangiogenic therapies in translational research of experimental tumours.

Keywords Angiogenesis; xenograft; nude mice; digital image analysis

Tumours, as any other tissue, require sufficient blood supply for the maintenance of metabolism and growth. While in small tumours of less than 1 mm diameter, the delivery of oxygen and nutrients is supported by diffusion from the surrounding tissue, larger tumours depend on a sufficient vasculature. It is now well accepted that tumours induce and maintain a specific tumour vasculature with sprouting of new capillary vessels from pre-existing vasculature. Neovascularization within an adult organism (angiogenesis) is slightly different from the original formation of vessels during embryonal or fetal development (vasculogenesis) (Risau 1997).

Correspondence: C Pöttgen, Department of Radiotherapy, University of Duisburg-Essen Medical School, Hufeland-strasse 55, D-45122 Essen, Germany.
Email: christoph.poettgen@uni-essen.de

Angiogenesis is induced and regulated by various growth receptors and proteins including vascular endothelial growth factor (VEGF)-family members (PIGF, VEGF A-D), Tie-2, PDGF, and integrins (Carmeliet & Jain 2000, Yancopoulos *et al*. 2000). The autocrine secretion of these factors is promoted by hypoxic conditions in the tumour microenvironment (Dor & Keshet 1997).

Neovascularization is a dynamic and complex process that is essential not only for primary tumour growth but also for metastatic disease. Based on the hypothesis that invasive growth and the potential for metastasis of solid tumours is dependent on the formation of their own vasculature, active inhibition of the angiogenic process seems to hold great promise as a therapeutic strategy, either alone or in combination with other antitumour therapies (Gong *et al*. 2003). However, little is known about the

functional status of microvessels generated during very early tumour formation and with increasing availability of anti-angiogenic agents, reliable methods that allow the preclinical evaluation of the effects on vascular pathophysiology in the tumour microenvironment, especially in *in vivo* models, are needed.

Therefore, we investigated the morphological and functional changes during neovascularization of growing tumours, using immunohistochemistry and digital image analysis as appropriate tools. These methods allow evaluation of relative vessel area and perfusion as a measure of the functional status of the vasculature at the same time.

Material and methods

Animals

Female nude mice (HsdCpb:NMRI*nu/nu*) were used in this study which are characterized by agenesis of the thymus. The lack of thymus-dependent T lymphocytes results in an immunodeficiency which allows the transplantation of human xenograft tumours. The mice were obtained from the Central Animal Laboratory of the University Duisburg-Essen Medical School, where breeding was performed under specific pathogen-free (SPF) conditions (barrier). The health status of the animals was investigated quarterly in accordance with the Federation of European Laboratory Animal Science Associations (FELASA) recommendations (Nicklas *et al*. 2002). Animals were free from pathogenic agents. Animals were housed at the Department of Radiation Oncology under filter-top cages in laminar air-flow units. They had unlimited access to water, supplemented with potassium sorbate (0.8 g/L) acidified to a pH of 3, and a high caloric nude mouse diet (12 ZH 10, Altromin, Germany). Animals were 6–9 weeks old when entering the experiment. All experiments were in accordance with animal protection laws and approved by the local study review board.

Tumour cell implantation

We used a human spindle cell sarcoma (ES3), which was originally derived from a biopsy of a patient's primary tumour and maintained by repeated transplantation to nude mice. Regular DNA analyses were accomplished to ascertain the human origin of the xenografts. The median doubling time of the tumour is 2.2 days. Cell suspensions (1.4×10^6 cells) were injected subcutaneously into the right hind leg. Tumours were grown without constraint, tumour size was measured every day using two perpendicular diameters. Tumour volume was calculated using the formula $V = a \times b^2/2$, with V = volume and a, b the long and short diameters, respectively. At predefined time points (days 3, 6, 10, 12, 13 and 14), a perfusion marker was given intravenously and tissue specimens from the tumour region were excised for further analyses after animals had been euthanized (see below).

Immunohistochemistry

As a marker of perfusion, Hoechst 33342 (0.2 mL in phosphate-buffered saline (PBS) solution, 7 mg/kg) was injected *in vivo* via the tail vein. Mice were anaesthetized with inhalation of ether and killed 5 min after injection by decapitation. Tumours were excised together with surrounding tissue and frozen sections of 6 μm thickness were cut. After fixation in acetone, rehydration with PBS was performed. Subsequently, tumours were incubated with the monoclonal rat anti-mouse 9F1-endothelial antibody (kindly provided by the Department of Pathology, University of Nijmegen, The Netherlands) for 225 min (at 4°C) in order to achieve adequate binding to the tumour vessels. The vasculature was then stained with a tetramethyl rhodamine iso-thiocyanate (TRITC)-labelled secondary (goat anti-rat) antibody (Tago, Burlingame, CA, USA) (Bernsen *et al*. 1995). Consecutive sections of the tumour region were paraffin-embedded, haematoxylin and eosin (HE)- and Giemsa-stained and examined using light microscopy (Zeiss Axioskop, Jena, Germany).

The occurrence of apoptotic cells in tissue sections and necrosis was analysed by terminal deoxy transferase uridine triphosphate nick-end labeling (TUNEL)

assay as described previously (Gavrieli *et al.* 1992). Following fixation, specimens were washed in PBS and incubated with terminal deoxynucleotidyl transferase (TdT enzyme) (ApopTag®, Oncor Inc, Gaithersburg, MD, USA). After fluorescent (fluorescein isothiocyanate [FITC]) staining, sections were counterstained with propidium iodide. Samples were examined by fluorescence microscopy (excitation: 490 nm, emission 520 nm).

Digital image analysis

Antibody-labelled sections of the tumours were evaluated by fluorescence microscopy (Zeiss Axioskop, Jena, Germany) and automated image analysis (Imtronic, Berlin, Germany). For analyses of vascular patterns, a 510–560 nm excitation filter and a 590 nm emission filter were used. Hoechst 33342 could be visualized (blue) in ultraviolet light using a 365 nm excitation and 420 nm emission filter in the same sections. Each tumour section was scanned completely with a fluorescence microscope using both filters subsequently. Digital image analysis (Imtronic Inc, Germany) allowed exact allocation of all separate fields (using 10 × objective) so that one large image could be reconstructed from all separately processed images. Artefacts were excluded manually by the investigator, and areas of necrosis were not included in further analyses. The fluorescence signals were then binarized (red and blue) after setting threshold values resulting in two composite images, one representing the vascular structures and another indicating the perfused areas. Matching of both images resulting in overlapping structures represented those vascular structures which were perfused by Hoechst at the time of injection. Quantitative analysis indicated relative vascular area: vascular area divided by total tumour area, as well as the fraction of perfused vessels: the amount of perfused vessels in proportion to the total vascular area, thus leading to distinct evaluation of morphological and functional conditions of the tumour microenviroment. Sections of normal subcutaneous tissue were investigated as controls.

Statistical analysis

Animals were randomly assigned to groups of seven mice per time point (tumour-bearing animals: 4, controls: 3). Quantitative analysis and statistical evaluation of vascular area and perfusion were performed using an individualized software program (based on EXCEL® and Visual Basic®, Microsoft Inc). Means and standard errors were calculated by the SAS software package (SAS Inc, Calgary, TX, USA). Differences were analysed using the *t*-test.

Results

Three days after implantation of tumour cells, agglomeration of tumour cells with high numbers of mitotic figures were observed in paraffin sections. This early tumour formation was accompanied by central areas of necrosis. A number of cells showed marked positivity in the TUNEL assay corresponding to apoptotic and necrotic cell loss.

At day 6, tumour formation was consolidated and invasion of granulocytic cells, e.g. macrophages, from the peripheral stromal tissue were observed (Figures 1–3).

At this time point, the digital image analysis revealed formation of vessels and perfusion was intensified around the tumour region (Figures 4a and b). The relative vascular area of the tumour region increased from 3.9% (SE ± 0.5) at day 3 up to 8.1% (SE ± 0.9) at day 6 ($P \leqslant 0.01$, two-sided *t*-test).

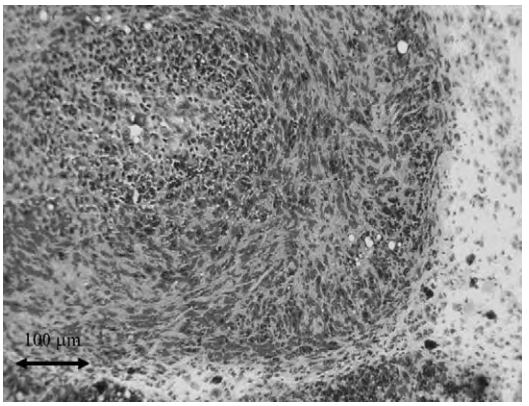

Figure 1 Haematoxylin/eosin-stained section of the tumour area, day 3, magnification 10 ×

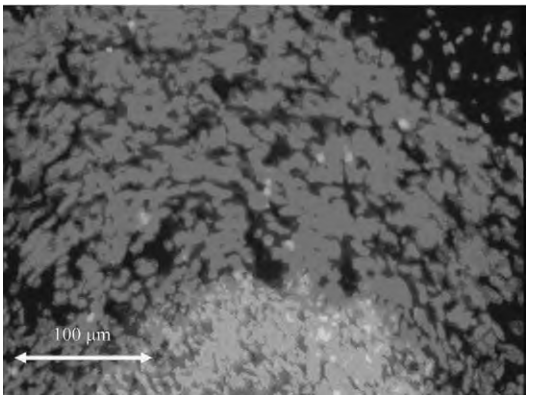

Figure 2 Corresponding section to Figure 1, terminal deoxy transferase uridine triphosphate nick-end labeling (TUNEL) assay, day 6, magnification 30 ×: viable cells show red fluorescence

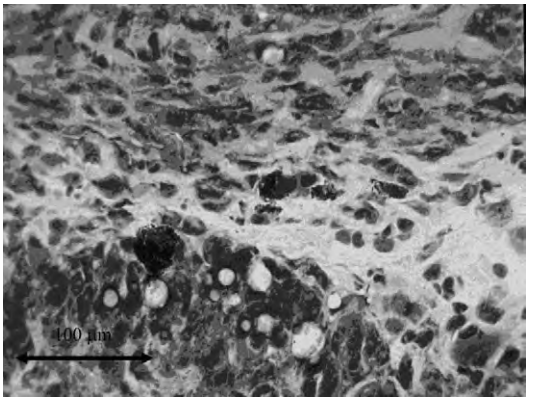

Figure 3 Detail of Figure 1, peripheral zone, day 6, magnification 30 ×: invasion of granulocytic cells

Perfusion, accounting for only 22.8% (SE ± 3.6) of vessels at day 3, reached a peak at day 6 with values around 52% (SE ± 3.1) of perfused vessels ($P \leqslant 0.01$, *t*-test, Figure 4c). During the following days, the tumour formation was further accomplished. After day 10, the tumour was fully integrated into the surrounding healthy tissue. At day 12, vascularity and perfusion decreased with values around 2.3% (SE ± 0.2) and 17.1% (SE ± 3.3), respectively. However, both parameters remained on a slightly higher level than the surrounding tissue of the host (Figure 5).

During the time course of the investigation, the region of interest (comprising the tumour area and a rim of connective tissue of the host) increased from 6 mm^2 (SE ± 0.22) at day 3 to 25.35 mm^2 (SE ± 3.58) at day 12.

Discussion

Several *in vivo* models have been used to investigate both morphological and functional aspects of the vascular system in xenotransplanted tumours (Gimbrone *et al.* 1974, Knighton *et al.* 1977, Lauk *et al.* 1989, Steinberg *et al.* 1990, Leunig *et al.* 1992, Passaniti *et al.* 1992). Microvascular corrosion casting is an excellent morphometric method for three-dimensional analysis of the vascular network and has been used to examine quantitatively time-dependent changes in the vascularity of the chick chorioallantoic membrane (Dimitropoulou *et al.* 1998). Moreover, corrosion casts have revealed significant quantitative differences in interbranch and intervessel distances related to a characteristic vascular architecture of various tumour types (Konerding *et al.* 1999). These differences were not dependent on the size or growth rate but rather on features characteristic of the cell type of the used experimental tumours. However, it has been found difficult to concurrently investigate the functional status of microvessels and morphometric parameters. Only few data are available, despite the fact that the functional status of a vascular network may have major biological impact on the sensitivity of a tumour towards cytotoxic drugs or irradiation. Tumour angiogenesis shows several structural and functional abnormalities including irregular branching patterns, increased vascular permeability and high amounts of arterio-venous shunt formation which leads to an inadequate perfusion (Thews *et al.* 2004).

However, objective evaluation of tumour vascularization has been hampered by difficulties in obtaining reproducible quantitative data. Computer-assisted image analysis offers advantages as a rapid and objective method for the quantitative

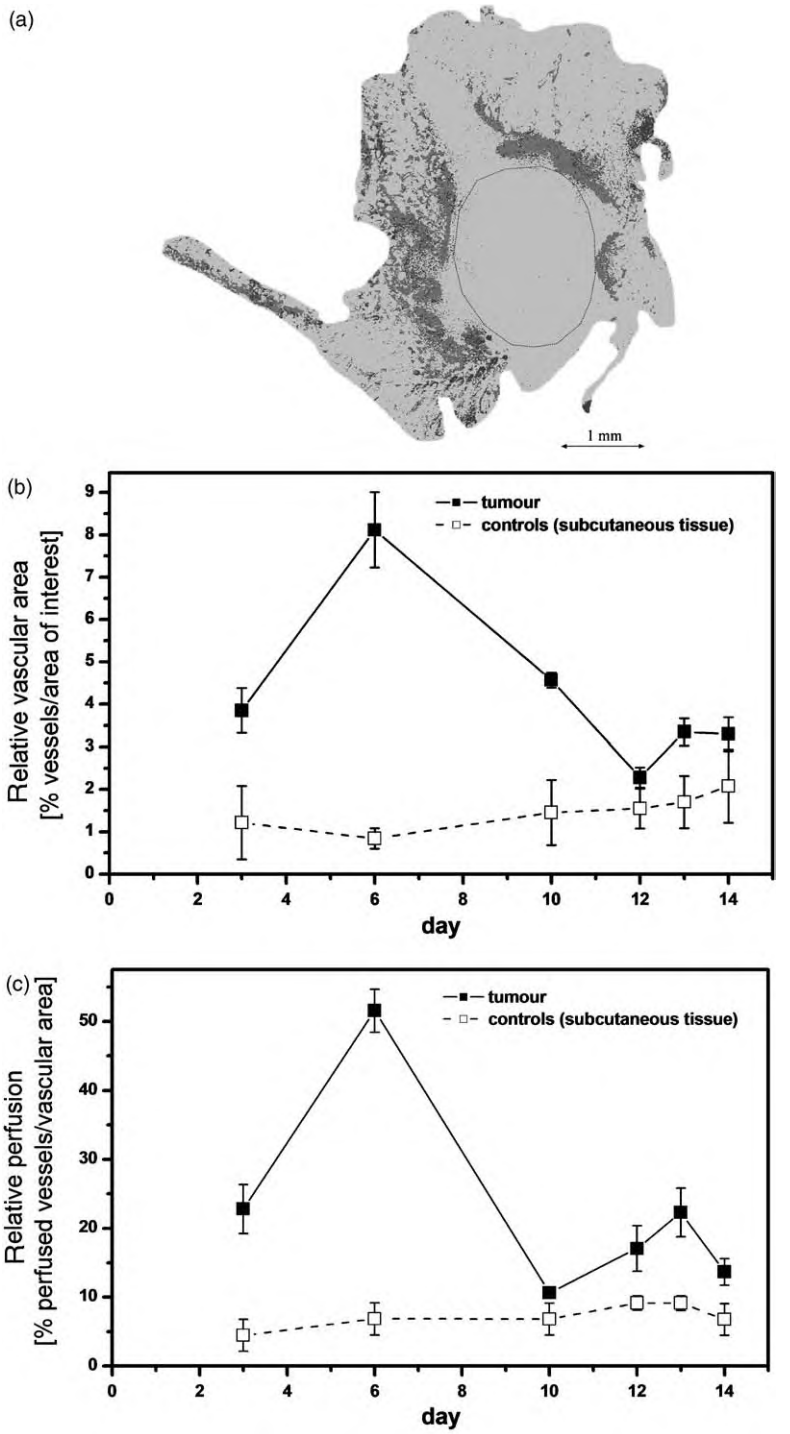

Figure 4 Vascularization and perfusion around the tumour. (a) Digitized (binary) image of tumour area at day 6, red = vasculature, blue = perfusion, magnification10 ×. (b) Relative vascular area: vascular area divided by tumour area, bars = standard error of the mean. (c) Amount of perfused vessels corresponding to perfused vessels divided by all vessels per tumour area

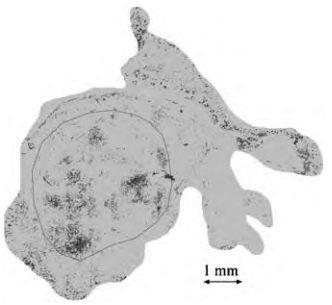

Figure 5 Digitized (binary) image of tumour area at day 14, red = vascular area, blue = perfusion, magnification 10 ×

assessment of vessel architecture (Wild *et al.* 2000). Chantrain *et al.* (2003) have employed a method of high-resolution slide scanning of whole tumour sections. They were able to analyse the endothelial area with high reproducibility by immunohistochemistry methods. However, no information about the functional status of the vasculature was provided.

Therefore, the combination of immunohistochemistry and digital image analysis, which allows simultaneous visualization of vascular patterns and perfusion together with quantitative assessment of vessel density (Bernsen *et al.* 1995, Bussink *et al.* 1998), has been developed. In the present study, this method was applied to analyse the tumour microenvironment after xenograft implantation of a human spindle cell sarcoma. The results indicate that tumour nutrition by diffusion from the host tissue is only sufficient for 3–4 days. Successful xenograft implantation is dependent on the tumour cell ability to induce angiogenesis (Hanahan & Folkman 1996, Denekamp *et al.* 1998). There is evidence that a significant amount of vessel formation is promoted during tumour growth, but establishing a solid tumour is accompanied by rising perfusion towards the tumour-bearing tissue area. Only selected cell lines will be able to maintain a functionally sufficient vascular network and establish a solid tumour *in vivo*. We observed functional vasculature in our human sarcoma xenograft model after 10–12 days from the day of injection of a cell suspension. In addition, our observations indicate that successful implantation of a xenografted tumour induces perfusion within the newly formed vascular network, which is directed towards the area of proliferating cells. With an increasing area occupied by the tumour, the relative vascular area decreases and the observed peak of relative amount of perfused vessels decreases after day 6.

It has recently been shown that the vasculature of experimental xenograft tumours may be influenced by microenvironmental factors. Using a rodent dorsal skinfold chamber model, Li *et al.* (2000) were able to demonstrate that tumour cells exhibit a chemotaxis-like migration toward the host blood vessels before the onset of angiogenesis. They observed an intimate relationship between the tumour cells and tumour neovasculature, with a process of unidirectional cell division and a close longitudinal alignment of tumour cells along the newly formed microvessels. They suggest that the identification of the responsible chemotactic signals would provide valuable targets for preventing tumour progression and metastasis.

Microregional variations depending on specific implantation sites may influence the growth of experimental xenografts. This applies, in particular, for tumours such as gliomas or prostate cancer cell lines which need a specific microenvironment in terms of surrounding stromal tissue or neuroendocrine stimuli, respectively (Bernsen *et al.* 1999, Gray *et al.* 2004). However, angiogenesis has been shown to be stimulated by hypoxia and consecutive upregulation of proangiogenic factors including VEGF. A series of excellent experiments has recently provided evidence for a two-stage model of tumour angiogenesis (Cao *et al.* 2005). The first phase occurs independent of hypoxia, while the consecutive hypoxia response appears to stimulate an even more intensive angiogenesis at a later stage. Consequently, the suppression of the hypoxia response may not be sufficient to inhibit the progress of incipient tumour angiogenesis.

Much attention has been given to the development of agents that inhibit angiogenesis in the clinic. VEGF is the ligand of at least two tyrosine-kinase receptors (Flt-1 and Flk-1/KDR). Recombinant humanized monoclonal antibodies that inhibit the binding of VEGF to the endothelial cell receptors have been shown to inhibit angiogenesis in animal models and are now being used in clinical trials (Prewett *et al*. 1999, Kabbinavar *et al*. 2003). Furthermore, antiangiogenic effects are potentiated by irradiation. Our group has demonstrated that the combination of specific or non-specific antiangiogenic agents (i.e. 2-methoxyestradiol, arginine deiminase) with irradiation leads to a reduction in the absolute number of tumour vessels and of perfused tumour vessels (Gong *et al*. 2003).

Although this study is limited to one single experimental tumour, the present nude mouse model appears suitable for providing an insight into the functional status of a vascular network and represents an excellent tool for studying even small tumours during early growth. Angiogenesis as well as the effects of antiangiogenic therapies can be investigated prospectively with regard to tumour microenvironment, morphology and functional changes.

Acknowledgements We thank Michael Groneberg, Kai Knühmann and Ingo Haase for excellent technical assistance with animal care and digital image analysis. This study was carried out at the Department of Radiotherapy, University of Duisburg-Essen Medical School, Essen, Germany.

References

Bernsen HJJA, Rijken PFJW, Hagemeier NEM, van der Kogel AJ (1999) A quantitative analysis of vascularization and perfusion of human glioma xenografts at different implantation sites. *Microvascular Research* **57**, 244–57

Bernsen HJJA, Rijken PFJW, Oostendorp T, van der Kogel AJ (1995) Vascularity and perfusion of human gliomas xenografted in the athymic nude mouse. *British Journal of Cancer* **71**, 721–6

Bussink J, Kaanders JHAM, Rijken PFJW, Martindale CA, van der Kogel AJ (1998) Multiparameter analysis of vasculature, perfusion and proliferation in human tumour xenografts. *British Journal of Cancer* **77**, 57–64

Cao Y, Li CY, Moeller BJ, *et al.* (2005) Observation of incipient tumor angiogenesis that is independent of hypoxia and hypoxia inducible factor-1 activation. *Cancer Research* **65**, 5498–505

Carmeliet P, Jain RK (2000) Angiogenesis in cancer and other diseases. *Nature* **407**, 249–57

Chantrain CF, DeClerck YA, Groshen S, McNamara G (2003) Computerized quantification of tissue vascularization using high-resolution slide scanning of whole tumor sections. *Journal of Histochemistry and Cytochemistry* **51**, 151–8

Denekamp J, Dasu A, Waites A (1998) Vasculature and microenvironmental gradients: the missing links in novel approaches to cancer therapy? *Advances in Enzyme Regulation* **38**, 281–99

Dimitropoulou C, Malkusch W, Maragoudakis ME, Konerding MA (1998) The vascular architecture of the chick chorioallantoic membrane: sequential quantitative evaluation using corrosion casting. *Angiogenesis* **2**, 255–63

Dor Y, Keshet E (1997) Ischemia-driven angiogenesis. *Trends in Cardiovascular Medicine* **7**, 289–94

Gavrieli Y, Sherman Y, Ben-Sasson SA (1992) Identification of programmed cell death *in situ* via specific labeling of nuclear DNA fragmentation. *Journal of Cell Biology* **119**, 493–501

Gimbrone MAJ, Cotran RS, Leapman SB, Folkman J (1974) Tumour growth and neovascularization: an experimental model using the rabbit cornea. *Journal of the National Cancer Institute* **52**, 413–27

Gong H, Pöttgen C, Stüben G, Havers W, Stuschke M, Schweigerer L (2003) Arginine deiminase and other antiangiogenic agents inhibit unfavorable neuroblastoma growth: potentiation by irradiation. *International Journal of Cancer* **106**, 723–8

Gray DR, Huss WJ, Yau JM, *et al.* (2004) Short-term human prostate primary xenografts: an *in vivo* model of human prostate cancer vasculature and angiogenesis. *Cancer Research* **64**, 1712–21

Hanahan D, Folkman J (1996) Patterns and emerging mechanisms of the angiogenic switch during tumorigenesis. *Cell* **86**, 353–64

Kabbinavar F, Hurwitz HI, Fehrenbacher L, *et al.* (2003) Phase II, randomized trial comparing bevacizumab plus fluorouracil (FU)/leucovorin (LV) with FU/LV alone in patients with metastatic colorectal cancer. *Journal of Clinical Oncology* **21**, 60–5

Knighton D, Ausprunk D, Tapper D, Folkman J (1977) Avascular and vascular phases of tumour growth in the chick embryo. *British Journal of Cancer* **35**, 347–56

Konerding MA, Malkusch W, Klapthor B, *et al.* (1999) Evidence for characteristic vascular patterns in solid tumours: quantitative studies using corrosion casts. *British Journal of Cancer* **80**, 724–32

Lauk S, Zietman A, Skates S, Fabian R, Suit HD (1989) Comparative morphometric study of tumour vasculature in squamous cell carcinomas in their

xenotransplants in athymic nude mice. *Cancer Research* **49**, 4557–61

Leunig M, Yuan F, Menger MD, *et al.* (1992) Angiogenesis, microvascular architecture, microhemodynamics, and interstitial fluid pressure during early growth of human adenocarcinoma LS174 T in SCID mice. *Cancer Research* **52**, 6553–60

Li CY, Shan S, Huang Q, *et al.* (2000) Initial stages of tumor cell-induced angiogenesis: evaluation via skin window chambers in rodent models. *Journal of the National Cancer Institute* **92**, 143–7

Nicklas W, Baneux P, Boot R, *et al.* (2002) Recommendations for the health monitoring of rodent and rabbit colonies in breeding and experimental units. *Laboratory Animals* **36**, 20–42

Passaniti A, Taylor RM, Pili R, *et al.* (1992) Methods in laboratory investigation. A simple, quantitative method for assessing angiogenesis and antiangiogenic agents using reconstituted basement membrane, heparin, and fibroblast growth factor. *Laboratory Investigations* **67**, 519–28

Prewett M, Huber J, Li Y, *et al.* (1999) Antivascular endothelial growth factor receptor (fetal liver kinase 1) monoclonal antibody inhibits tumor angiogenesis and growth of several mouse and human tumors. *Cancer Research* **59**, 5209–18

Risau W (1997) Mechanisms of angiogenesis. *Nature* **386**, 671–4

Steinberg F, Konderding MA, Streffer C (1990) The vascular architecture of human xenotransplanted tumours, histological, morphometrical, and ultrastructural studies. *Journal of Cancer Research and Clinical Oncology* **116**, 517–24

Thews O, Wolloscheck T, Dillenburg W, *et al.* (2004) Microenvironmental adaptation of experimental tumours to chronic vs acute hypoxia. *British Journal of Cancer* **91**, 1181–9

Wild R, Ramakrishnan S, Sedgewick J, Griffioen AW (2000) Quantitative assessment of angiogenesis and tumor vessel architecture by computer-assisted digital image analysis: effects of VEGF-toxin conjugate on tumor microvessel density. *Microvascular Research* **59**, 368–76

Yancopoulos GD, Davis S, Gale NW, Rudge JS, Wiegand SJ, Holash J (2000) Vascular-specific growth factors and blood vessel formation. *Nature* **407**, 242–8